The behavior of the *I-V-T* characteristics of inhomogeneous (Ni/Au)–$Al_{0.3}Ga_{0.7}N$/AlN/GaN heterostructures at high temperatures

Z. Tekeli, Ş. Altındal, M. Çakmak,[a] and S. Özçelik
Physics Department, Faculty of Arts and Sciences, Gazi University, Ankara 06500, Turkey

D. Çalışkan and E. Özbay
Nanotechnology Research Center, Bilkent University, Bilkent, Ankara 06800, Turkey;
Department of Physics, Bilkent University, Bilkent, Ankara 06800, Turkey;
and Department of Electrical and Electronics Engineering, Bilkent University, Bilkent, Ankara 06800, Turkey

(Received 28 May 2007; accepted 20 July 2007; published online 12 September 2007)

We investigated the behavior of the forward bias current-voltage-temperature (*I-V-T*) characteristics of inhomogeneous (Ni/Au)–$Al_{0.3}Ga_{0.7}N$/AlN/GaN heterostructures in the temperature range of 295–415 K. The experimental results show that all forward bias semilogarithmic *I-V* curves for the different temperatures have a nearly common cross point at a certain bias voltage, even with finite series resistance. At this cross point, the sample current is temperature independent. We also found that the values of series resistance (R_s) that were obtained from Cheung's method are strongly dependent on temperature and the values abnormally increased with increasing temperature. Moreover, the ideality factor (n), zero-bias barrier height (Φ_{B0}) obtained from *I-V* curves, and R_s were found to be strongly temperature dependent and while Φ_{B0} increases, n decreases with increasing temperature. Such behavior of Φ_{B0} and n is attributed to Schottky barrier inhomogeneities by assuming a Gaussian distribution (GD) of the barrier heights (BHs) at the metal/semiconductor interface. We attempted to draw a Φ_{B0} versus $q/2kT$ plot in order to obtain evidence of the GD of BHs, and the values of $\bar{\Phi}_{B0}=1.63$ eV and $\sigma_0=0.217$ V for the mean barrier height and standard deviation at a zero bias, respectively, were obtained from this plot. Therefore, a modified $\ln(I_0/T^2)-q^2\sigma_0^2/2(kT)^2$ versus q/kT plot gives Φ_{B0} and Richardson constant A^* as 1.64 eV and 34.25 $A/cm^2\,K^2$, respectively, without using the temperature coefficient of the barrier height. The Richardson constant value of 34.25 $A/cm^2\,K^2$ is very close to the theoretical value of 33.74 $A/cm^2\,K^2$ for undoped $Al_{0,3}Ga_{0,7}N$. Therefore, it has been concluded that the temperature dependence of the forward *I-V* characteristics of the (Ni/Au)–$Al_{0.3}Ga_{0.7}$/AlN/GaN heterostructures can be successfully explained based on the thermionic emission mechanism with the GD of BHs. © *2007 American Institute of Physics*. [DOI: 10.1063/1.2777881]

I. INTRODUCTION

The attractive features of GaN and other related GaN-based materials have gained significant interest for use in the production of high-power/high frequency and high-temperature applications compared with conventional Si or GaAs related devices.[1–10] In order to fabricate reliable and high-performance electronic devices, it is still indispensable to clarify the electronic properties at metal/GaN and AlGaN interfaces because the true interface properties, such as the Schottky barrier formation and interfacial insulator layer, have sometimes been screened owing to nonreliable current-voltage and capacitance-voltage characteristics. On the free surfaces of GaN and AlGaN, high-density surface states exist, which cause charge-discharge transients in turn leading to performance instability, such as current collapse and poor long-term reliability. The formation of an interfacial insulator layer on a semiconductor by the traditional methods of oxidation or deposition cannot completely passivate the active dangling bonds at the semiconductor surface. A satisfactory surface passivation method to cope with these problems has not been established yet, although some encouraging results have been reported for the use of Si_3N_4 (Refs. 11–13) and Al_2O_3.[14] At the metal-semiconductor interfaces, Schottky barrier heights (SBHs) are much more dependent on the metal work function than other III-V materials,[15] which indicates a weaker pinning of the Fermi level. Although Schottky diodes formed on GaN and AlGaN materials exhibit excess reverse leakage currents that are many orders of magnitude larger than the prediction of the standard thermionic emission (TE) model, many researchers[16–21] analyze *I-V* characteristics based on the TE model.

Until now, a complete description of the current transport mechanism through a barrier, and understanding Schottky barrier formation and the insulation layer between the metal and semiconductor interface, still remains a challenging problem. In addition, the change in temperature has important effects on the determination of the main diode parameters such as barrier height (Φ_B), n, and R_s. The temperature dependence electrical characteristics of metal-semiconductor (MS) and metal-insulator-semiconductor (MIS) structures have been prevalent in the literature for

[a]Electronic mail: cakmak@gazi.edu.tr

more than four decades.[12,16–29] It is often found that the Φ_B extracted from the linear parts of semilogarithmic *I-V* characteristics, using the TE theory, increases and n decreases with increasing temperature. These changes are especially more significant at low temperatures of such behavior of Φ_B, and that n cannot be explained according to the standard TE theory.

The high values of n can be attributed to the effects of the bias voltage drop across the interface insulator layer and R_s, and therefore, of the bias voltage dependence of the barrier height.[20,28,29] Werner and Güttler[28,29] suggested a distribution of Schottley Barrier Diodes (SBDs) as a result of special inhomogeneities at the metal/semiconductor interface. According to this model, the deviation of n from unity and its temperature dependence on the barrier distribution are due to the voltage dependence of the barrier distribution. In addition, the forward bias *I-V* characteristics at the high voltage region ($V \geqslant 0.6$ V) deviate considerably from linearity due to the series resistance R_s and insulation layer. The R_s parameter is effective especially in the downward curvature region of forward bias *I-V* characteristics. In the literature, several methods were suggested in order to extract R_s from MS or MIS SBDs.[30–32] However, they suffer from a limitation of their applicability for practical devices with an interfacial insulator layer. Norde[30] proposed a method for the evaluation of R_s from the forward *I-V* characteristics, in which an ideal Schottky diode was sought, namely, with $n=1$. For $n>1$, Sato and Yasamona[31] used a function $F(V)$ similar to that of Norde, taking into account that n can be greater than unity. We used a method developed by Cheung and Cheung[32] in order to obtain the R_s values.

In the present study, the electrical characteristics of $(Ni/Au)-Al_{0.3}Ga_{0.7}N/AlN/GaN$ heterostructures were studied in the temperature range of 295–415 K. Φ_B, n, and R_s were extracted from the forward bias *I-V* measurements. The R_s parameter was estimated from Cheung and Cheung's method,[32] and was strongly temperature dependent and abnormally increased with increasing temperature. The temperature dependence of SBH characteristics of $(Ni/Au)-Al_{0.3}Ga_{0.7}N/AlN/GaN$ heterostructures are interpreted based on the existence of the Gaussian distribution (GD) of the BHs around a mean value due to the barrier height inhomogeneities prevailing at the metal-semiconductor interface.

II. EXPERIMENTAL DETAILS

The $Al_{0.3}Ga_{0.7}N/AlN/GaN$ heterostructure with a high-temperature (HT) AlN buffer layer (BL) that was investigated in the present study was grown on *c*-face sapphire (Al_2O_3) substrate by low-pressure metal-organic chemical-vapor deposition (MOCVD). Hydrogen was used as the carrier gas and trimethylgallium (TMGa), trimethylaluminum (TMAl), and ammonia (NH_3) were used as source compounds. Prior to the epitaxial growth, Al_2O_3 substrate was annealed at 1100 °C for 10 min to remove surface contamination. As shown in Fig. 1, a 15-nm-thick AlN nucleation layer was first deposited on Al_2O_3 substrate at 840 °C. Then, the reactor temperature was ramped to 1150 °C and a HT AlN BL was grown, followed by 2 min growth interruption in order to reach growth conditions for GaN. GaN BL was grown at a reactor pressure of 200 mbars, growth temperature of 1070 °C, and growth rate of approximately 2 μm/h. Then, for a sample, a 2-nm-thick HT AlN interlayer was grown at a temperature of 1085 °C and a pressure of 50 mbars. Finally, a 25-nm-thick AlGaN ternary layer and a 2-nm-thick GaN cap layer growth was carried out at a temperature of 1085 °C and a pressure of 50 mbars, respectively.

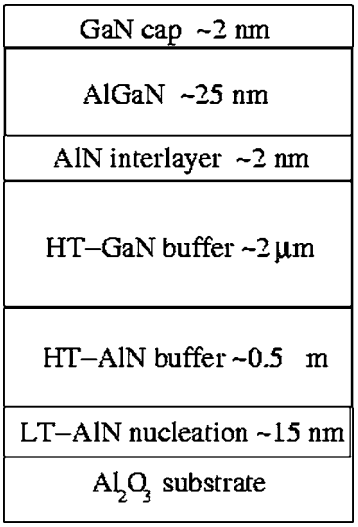

FIG. 1. Schematic diagram of the $Al_{0.3}Ga_{0.7}N/AlN/GaN$ heterostructure.

For the contacts, since the sapphire substrate is insulating, the Ohmic contacts and Schottky contacts were made atop the surface as 2 mm diameter circular dots. Prior to Ohmic contact formation, the samples are cleaned with acetone in an ultrasonic bath. Then, a sample is treated with boiling isopropyl alcohol for 5 min and rinsed in de-ionized (DI) water. After cleaning, the samples are dipped in a solution of HCl/H_2O (1:2) for 30 s in order to remove the surface oxides, and then rinsed in DI water again for a prolonged period. For the contact formation, Ti/Al/Ni/Au (200/2000/400/500 Å) metals are thermally evaporated on the sample. After the metallization step, the contacts are annealed at 850 °C for 30 s in N_2 ambient in order to form Ohmic contact. The formation of the Ohmic contact is followed by Ni/Au (350/500 Å) evaporation as Schottky contacts. Prior to Schottky metal deposition, the same cleaning procedure for the Ohmic contacts is used for cleaning the sample surface.

The current-voltage (*I-V*) measurements were performed by the use of a Keithley 220 programmable constant current source, and a Keithley 614 electrometer in the temperature range of 295–415 K using a temperature controlled Janes vpf-475 cryostat, which enabled us to perform measurements in the temperature range of 77–450 K. The sample temperature was always monitored by use of a copper-constant thermocouple close to the sample and measured with a Keithley model 199 DMM/scanner and Lake Shore model 321 autotuning temperature controllers with sensitivity better than ±0.1 K.

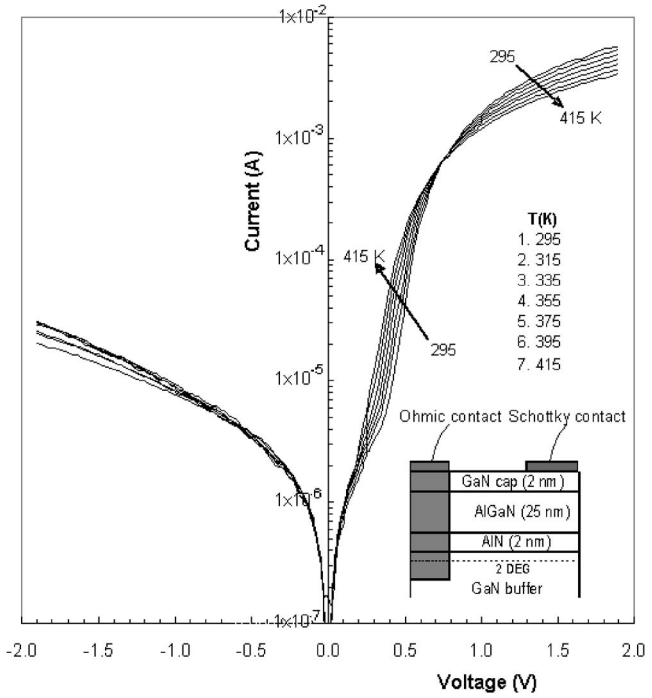

FIG. 2. Forward and reverse bias semilogarithmic *I-V* characteristics of a $(Ni/Au)-Al_{0.3}Ga_{0.7}N/AlN/GaN$ heterostructure at various temperatures.

III. RESULTS AND DISCUSSIONS

When a $(Ni/Au)-Al_{0.3}Ga_{0.7}N/AlN/GaN$ heterostructure with R_s is considered, the current through the junction can be given by the TE model for the relationship between the forward bias voltage and the current of SBDs and can be expressed as[20,21]

$$I = I_0 \exp\left[\frac{q(V - IR_s)}{nkT}\right]\left\{1 - \exp\left[\frac{-q(V - IR_s)}{kT}\right]\right\}, \quad (1)$$

where I_0 is the reverse saturation current derived from the straight line intercept of the current at a zero bias and is given by

$$I_0 = AA^*T^2 \exp\left(-\frac{q\Phi_{B0}}{kT}\right), \quad (2)$$

where the IR_s term is the voltage drop across the R_s of structure, in which A is the rectifier contact area, A^* is the effective Richardson constant (33.74 $A/cm^2\,K^2$ for undoped $Al_{0.3}Ga_{0.7}N$),[33] T is temperature in kelvin, k is the Boltzmann constant, q is the electronic charge, and Φ_{B0} is the apparent barrier height at zero bias. The ideality factor n is calculated from the slope of the linear region of the forward bias *I-V* plot and can be written as from Eq. (1),

$$n = \frac{q}{kT}\left(\frac{dV}{d\ln I}\right). \quad (3)$$

n is introduced to take into account the deviation of the experimental *I-V* data from the ideal TE theory and should be $n=1$ for an ideal contact. Figure 2 shows the forward bias semilogarithmic *I-V* characteristics of a $(Ni/Au)-Al_{0.3}Ga_{0.7}N/AlN/GaN$ heterostructure with GaN capping at various temperatures, ranging from 295 to 415 K. As can be seen in Fig. 2, the semilogarithmic *I-V* curves are linear between the intermediate bias region ($0.2 \leqslant V \leqslant 0.6$ V). The saturation current I_0 was obtained by extrapolating the linear intermediate voltage region of the part of the linear curve to a zero applied bias voltage for each temperature. The experimental values of Φ_{B0} and n were determined from Eqs. (2) and (3), respectively, and are reported in Table I and Fig. 3. As shown in Table I, the values of Φ_{B0} and n for the $(Ni/Au)-Al_{0.3}Ga_{0.7}N/AlN/GaN$ heterostructure ranged from 0.721 eV and 2.45 (at 295 K) to 0.989 eV and 1.89 (at 415 K), respectively. Our sample with a large value of n was attributed to the presence of a thick interfacial insulator layer between the metal and semiconductor.[12,17,18,20,21] As explained in Refs. 12 and 24–28, since the current transport

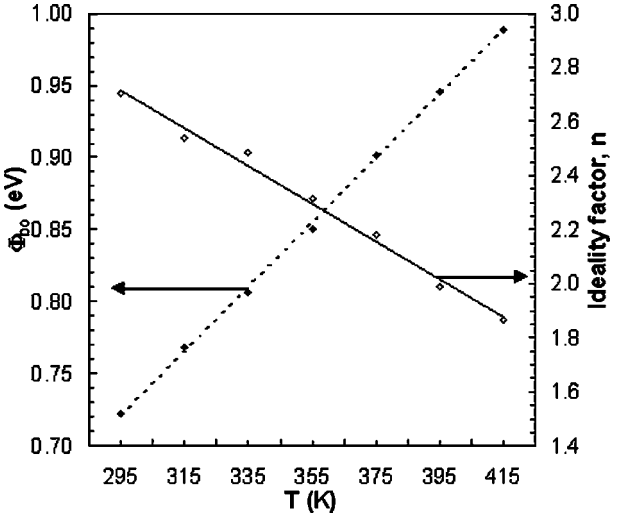

FIG. 3. The zero-bias barrier height Φ_{B0} and the ideality factor n of a $(Ni/Au)-Al_{0.3}Ga_{0.7}N/AlN/GaN$ heterostructure obtained from the forward bias *I-V* data at various temperatures.

TABLE I. Temperature dependent values of various parameters determined from the forward bias *I-V* characteristics of a $(Ni/Au)-Al_{0.3}Ga_{0.7}N/AlN/GaN$ heterostructure.

T (K)	I_0 (nA)	$n_{(I\text{-}V)}$	$n_{(dv/d\ln I)}$	$\Phi_{B_0(I\text{-}V)}$ (eV)	$\Phi_{B(H\text{-}I)}$ (eV)	$R_{s(dv/d\ln)}$ (Ω)	$R_{s(H\text{-}I)}$ (Ω)
295	35	2.70	2.45	0.72	0.84	177.44	195.48
315	45	2.53	2.34	0.77	0.95	217.01	248.58
335	58	2.48	2.04	0.81	1.03	249.12	286.15
355	75	2.31	1.75	0.86	1.04	281.03	328.44
375	93	2.17	1.23	0.90	1.13	317.52	368.20
395	113	1.98	1.05	0.95	1.19	356.61	411.27
415	144	1.89	1.02	0.99	1.23	394.11	457.89

across the metal-semiconductor interface is a temperature activated process, electrons at low temperatures are able to surmount the lower barriers. Therefore, the current transport will be dominated by the current flowing through the patches of lower SBHs.[19,22,30] Therefore, the value of n increases with decreasing temperature. In addition, as shown in Fig. 3, the values of Φ_{B0} of the (Ni/Au)–$Al_{0.3}Ga_{0.7}N$/AlN/GaN heterostructure calculated from the *I-V* characteristics show the unusual behavior of increasing with the increase of temperature. Such temperature dependence is an obvious disagreement with the reported negative temperature coefficient of the barrier height or forbidden band gap of a semiconductor (GaN or AlGaN).

As shown in Fig. 2, the forward bias *I-V* characteristics are linear in the intermediate bias regions ($0.2 \leqslant V \leqslant 0.6$ V) but deviate considerably from linearity due the R_s effect of a structure when the applied bias voltage is sufficiently large. R_s is significant in the downward curvature (at high bias voltages) of the forward bias *I-V* characteristics. As the linear range of the forward *I-V* plots is reduced, the accuracy of the determination of Φ_{B0} and n becomes poorer. Φ_B and other main electrical parameters, such as n and R_s, were achieved using a method developed by Cheung and Cheung.[31] Cheung and Cheung's functions

$$\frac{dV}{d\ln I} = IR_s + \left(\frac{nkT}{q}\right), \tag{4}$$

$$H(I) = V - \left(\frac{nkT}{q}\right)\ln\left(\frac{I}{AA^*T^2}\right) = IR_s + n\Phi_B \tag{5}$$

should give a straight line for the data of the downward curvature region in the forward bias *I-V* characteristics, where Φ_B is the barrier height obtained from the data of the downward curvature region in the forward bias *I-V* characteristics. The value of n calculated from the slope of the linear portion of the forward bias *I-V* characteristics especially includes the effect of the interfacial parameters such as n; Φ_B and R_s enable us to obtain Cheung and Cheung's functions.[32] Figures 4(a) and 4(b), experimental $dV/d\ln I$ versus I, and $H(I)$ versus I plots are presented at different temperatures of a (Ni/Au)–$Al_{0.3}Ga_{0.7}N$/AlN/GaN heterostructure, respectively. Therefore, n and R_s were determined from the intercept and slope of the $dV/d\ln I$ versus I plots [Fig. 4(a)] at each temperature. Thereafter, using the n value determined from Eq. (4) and the data of the downward curvature region in the forward bias *I-V* characteristics in Eq. (5), a plot of $H(I)$ versus I plots [Fig. 4(b)] will also lead to a straight line with a y-axis intercept that is equal to $n\Phi_B$. The slope of this plot also provides a second determination of R_s, which can be used to check the consistency of this approach. Therefore, for each temperature and by performing different plots [Eqs. (4) and (5)] of the *I-V* data, three main diode parameters (n, Φ_B, and R_s) are obtained and presented in Table I. As shown in Table I, the obtained n and R_s values by way of different techniques are in good agreement with each other.

As can be seen in Table I, there is an abnormal increase in the experimental values Φ_B and R_s with increasing temperature while n decreases with increasing temperature. In addition, as can be seen in Fig. 2, an interesting feature of the forward bias *I-V* curves is the nearly common intersection point of all the curves at a certain bias voltage, and for this voltage point, the current through the junction is temperature independent.

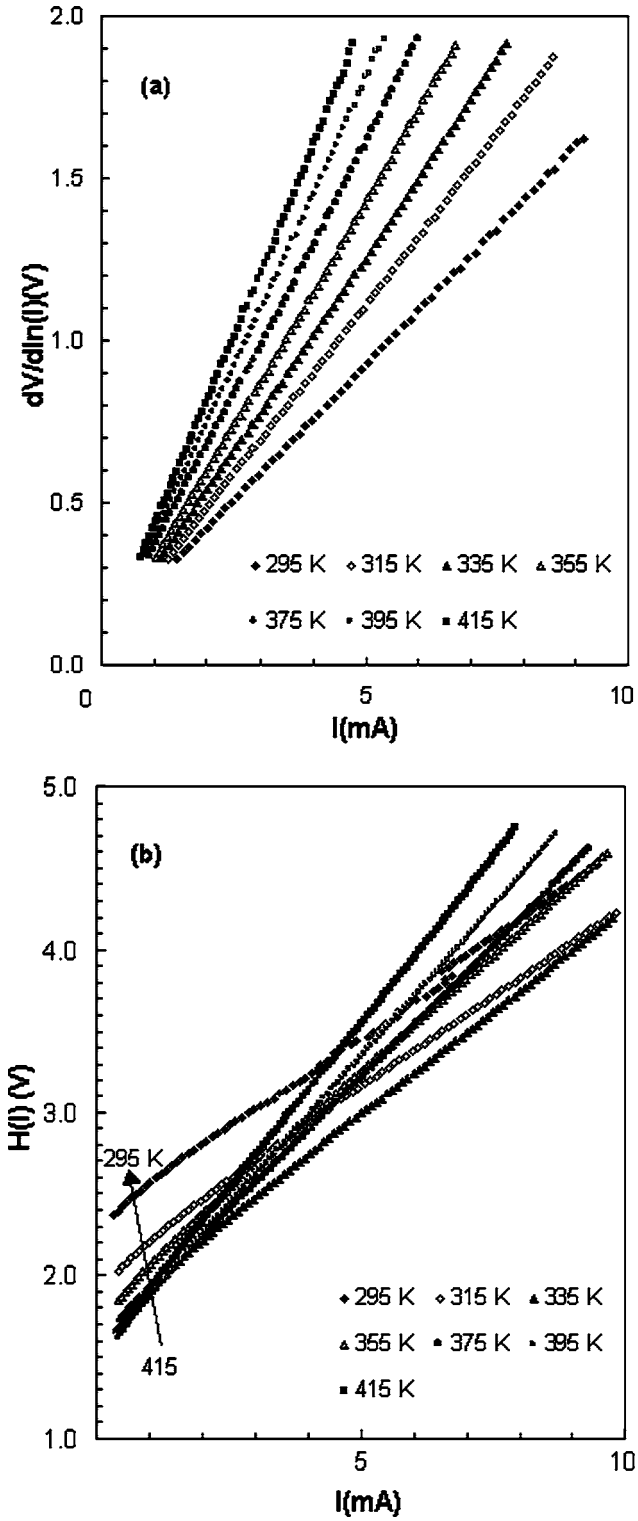

FIG. 4. The characteristics of the (Ni/Au)–$Al_{0.3}Ga_{0.7}N$/AlN/GaN heterostructure obtained from the forward bias *I-V* data at various temperatures: (a) $dV/d\ln I$ versus I and (b) $H(I)$ versus I.

Similar results have been obtained recently by simula-

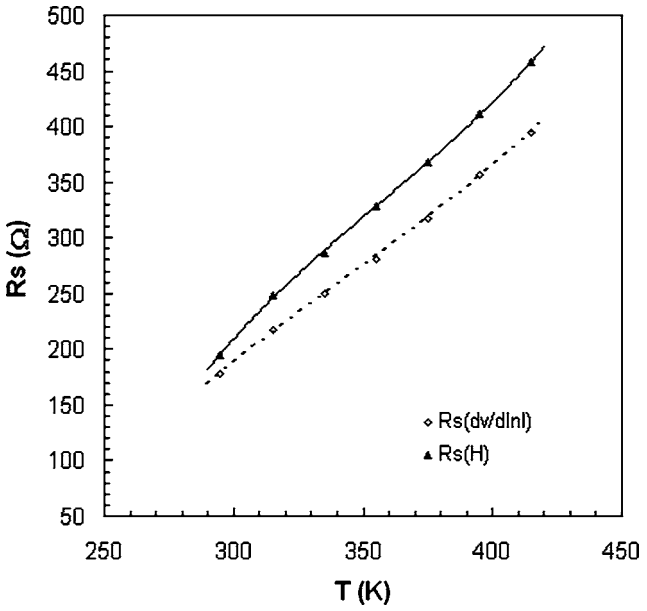

FIG. 5. The temperature dependence of R_s for the studied (Ni/Au)–$Al_{0.3}Ga_{0.7}N$/AlN/GaN heterostructure.

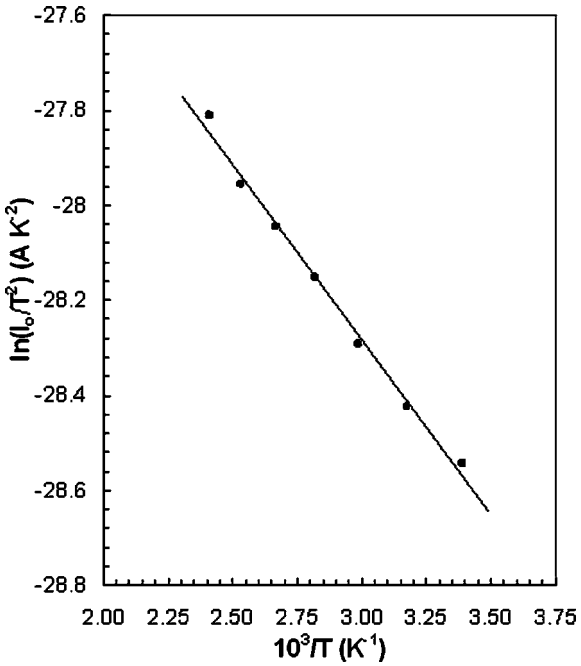

FIG. 6. Richardson plots of the $\ln(I_0/T^2)$ versus $10^3/T$ for (Ni/Au)–$Al_{0.3}Ga_{0.7}N$/AlN/GaN heterostructure.

tion of the forward bias *I-V* curves of Schottky diodes.[34–36] It was found that the presence of R_s in a device causes bending due to current saturation and plays a subtle role in keeping this intersection hidden. Additionally, Chand and Bala[35] reported that this intersection of forward bias *I-V* curves for a homogeneous Schotky diode can only be realized in curves with zero series resistance. Osvald[37] showed theoretically that the presence of R_s is a necessary condition of the intersection of the *I-V* curves. However, Horvath *et al.*,[38] Dökme and Altındal,[19] and Altındal *et al.*[39] reported that they found an intersection point in the forward bias *I-V* characteristics of an $Al/SiO_2/Si$ structure by way of experiments. This intersection behavior of the forward bias *I-V* curves appears as an abnormality when seen with respect to the conventional behavior of SBDs. The values of R_s versus temperature determined from Eqs. (4) and (5) are shown in Fig. 5. As can be seen in Fig. 5, R_s calculated from the Cheung and Cheung's function shows an unusual behavior wherein it increases with an increase in temperature. In general, such temperature dependence is an obvious disagreement with the reported negative temperature coefficient of R_s. Such behavior was attributed to the lack of free charge at a low temperature and in the temperature region where there is no carrier freezing out, which is only not negligible at a low temperature.[20] At higher temperatures, the contact resistance and resistance of the outer connections are probably the prevalent sources of R_s. A similar temperature dependence was obtained experimentally[40] and theoretically.[34]

A. Inhomogeneous barrier analysis

In order to extract the SBD parameters, the conventional TE theory is normally used.[12,16–18,20,21] However, there have been several reports about a deviation from this classical TE theory.[12,18–20,24–28,38–41] For the evaluation of the barrier height, one may also make use of the conventional activation energy plot of reverse saturation current. Equation (2) can be written as

$$\ln\left(\frac{I_0}{T^2}\right) = \ln(AA^*) - \frac{q\Phi_{B0}}{kT}. \tag{6}$$

The plot is found to be linear in the temperature range measured. The experimental data asymptotically fit to a straight line at a studied temperature range of 295–415 K. Activation energy and Richardson constant A^* values were determined from the slope and intercept at an ordinate of the linear region of the $\ln(I_0/T^2)$ versus $10^3/T$ plot (as seen in Fig. 6) as 0.064 eV and 1.52×10^{-10} A/cm^2 K^2, respectively. This value of the Richardson constant (A^*) is much lower than the known value of 33.74 A/cm^2 K^2 for electrons in undoped $Al_{0.3}Ga_{0.7}N$.

As was explained by Horvath,[42] the A^* value obtained from the temperature dependence of the *I-V* characteristics may be affected by the lateral inhomogeneity of the barrier. According to Refs. 12, 20, 26, 28, 29, 43, and 44, the ideality factor of an inhomogeneous SBDs with a distribution of low SBHs may increase with a decrease in temperature. Schmitsdorf *et al.*[44] used Tung's[45] theoretical approach and found a linear correlation between the experimental Φ_{B0} and n. Figure 7 shows a plot of the experimental Φ_{B0} versus n with temperature. The straight line shown in Fig. 7 is the least squares fit to the experimental data. As can be seen in Fig. 7, there is a linear relationship between the experimentally effective BHs and the ideality factors of the Schottky contact that was explained by the lateral inhomogeneities of the BHs in the Schottky diodes.[12,26,44] The extrapolation of the experimental BHs versus n plot to $n=1$ has given a homogeneous BH of approximately 1.85 eV. Therefore, it can be said that

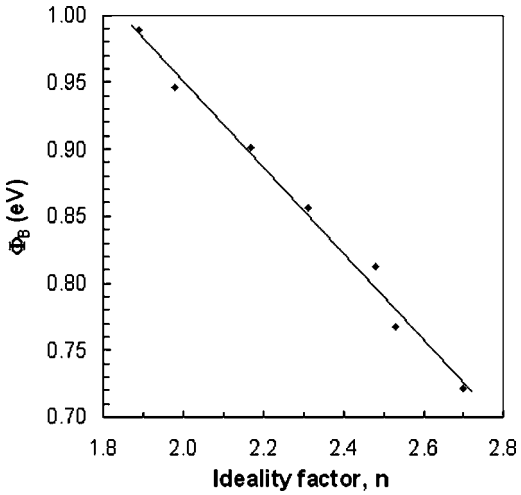

FIG. 7. Φ_B versus n of a typical (Ni/Au)–$Al_{0.3}Ga_{0.7}N$/AlN/GaN heterostructure at different temperatures.

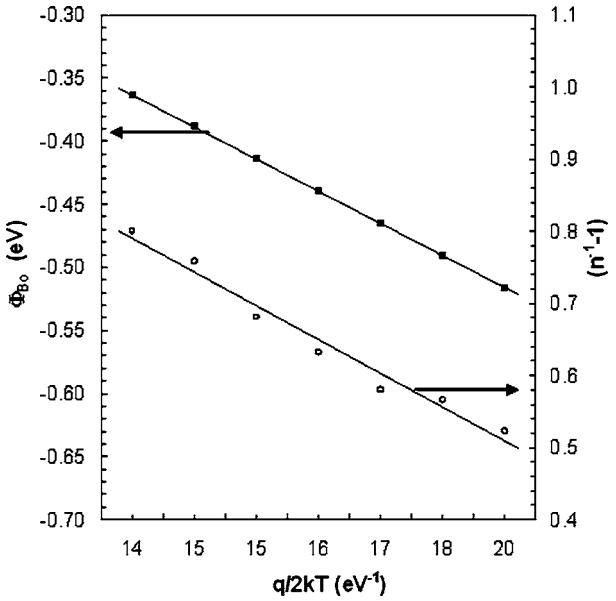

FIG. 8. Φ_{B0} and n ideality factor versus q/kT curves of a (Ni/Au)–$Al_{0.3}Ga_{0.7}N$/AlN/GaN heterostructure according to the GD of BHs.

a significant decrease of Φ_{B0} and an increase of n especially at a low temperature are possibly caused by the inhomogeneities of BHs.

In performing an analysis based on barrier inhomogeneity, we shall adopt the model of Werner and Güttler,[28,29] introducing a GD in BHs with a mean value $\bar{\Phi}_{B0}$ and standard deviation σ_s,

$$P(\Phi_B) = \frac{1}{\sigma_s\sqrt{2\pi}} \exp\left[-\frac{(\Phi_B - \bar{\Phi}_B)^2}{2\sigma_s^2}\right], \tag{7}$$

where $1/[\sigma_s(2\pi)^{1/2}]$ is the normalization constant of GD of the barrier height. The total current $I(V)$ across a Schottky diode containing barrier inhomogeneities can be expressed as

$$I(V) = \int_{-\infty}^{+\infty} I(\Phi_B, V)P(\Phi_B)d\Phi, \tag{8}$$

where $I(\Phi_B, V)$ is the current at a bias V for a barrier of height based on the ideal thermionic-emission-diffusion theory and $P(\Phi_B)$ is the normalized distribution function giving the probability of accuracy for the barrier height.

Performing this integration from $-\infty$ to $+\infty$, one can obtain the current $I(V)$ through a Schottky barrier at a forward bias, as in Eqs. (9) and (10). These equations are similar to Eqs. (1) and (2) but with the modified barrier,

$$I_0 = AA^*T^2 \exp\left(-\frac{q\Phi_{ap}}{kT}\right), \tag{9}$$

$$I(V) = A^*T^2 \exp\left[-\frac{q}{kT}\left(\bar{\Phi} - \frac{q\sigma_S^2}{2kT}\right)\right]\exp\left(\frac{qV}{n_{ap}kT}\right) \times\left\{1 - \exp\left[-\frac{q(V - IRs)}{kT}\right]\right\}, \tag{10}$$

where Φ_{ap} and n_{ap} are the apparent barrier height and apparent ideality factor, respectively, and are given by[12,26–28]

$$\Phi_{ap} = \bar{\Phi}_{B0}(T=0) - \frac{q\rho_0^2}{2kT}, \tag{11}$$

$$\left(\frac{1}{n_{ap}} - 1\right) = \rho_2 - \frac{q\rho_3}{2kT}. \tag{12}$$

It is assumed that the modified SBH $\bar{\Phi}_{B0}$ and σ_s are linearity bias dependent on Gaussian parameters, such as $\Phi_B = \bar{\Phi}_{B0} + \rho_2 V$ and the standard deviation $\sigma_s = \rho_{s0} + \rho_3 V$, where ρ_2 and ρ_3 are voltage coefficients that may depend on temperature and qualify the voltage deformation of the BH distribution.[12,26,27] The temperature dependence of σ_s is usually small and can be neglected.[26,44]

We attempted to draw a Φ_{B0} versus $q/2kT$ plot (as seen in Fig. 8) to obtain evidence of the GD of the BHs, and the values of $\bar{\Phi}_{B0} = 1.63$ eV and $\sigma_s = 0.217$ V for the mean barrier height and standard deviation at a zero bias, respectively, which have been obtained from this plot. The structure with the best rectifying performance presents the best barrier homogeneity with the lower value of the standard deviation. It was seen that the value of $\sigma_0 = 0.217$ V is not small compared to the mean value values of $\bar{\Phi}_{B0} = 1.63$ eV, and it indicates the presence of the interface inhomogeneities. Therefore, the plot of $[(1/n_{ap}) - 1]$ versus $q/2kT$ should be a straight line that gives the voltage coefficients ρ_2 and ρ_3 from the intercept and slope, respectively (as shown in Fig. 8). The values of $\rho_2 = -0.095$ V and $\rho_3 = -0.028$ V were obtained from the experimental $[(1/n_{ap}) - 1]$ versus $q/2kT$ plot.

Now, combining Eqs. (10) and (11) we get

$$\ln\left(\frac{I_0}{T^2}\right) - \left(\frac{q^2\rho_0^2}{2k^2T^2}\right) = \ln(AA^*) - \frac{q\bar{\Phi}_{B0}}{kT}. \tag{13}$$

The plot of a modified $\ln(I_0/T^2) - q^2\sigma_0^2/2k^2T^2$ versus q/kT plot according to Eq. (13) should give a straight line with the slope directly yielding the mean $\bar{\Phi}_{B0}$ as 1.64 eV and the intercept $(=\ln AA^*)$ at the ordinate determining A^* for a given diode area A as 34.25 A/cm^2 K^2 (as seen in Fig. 9), respectively, without using the temperature coefficient of the SBHs.

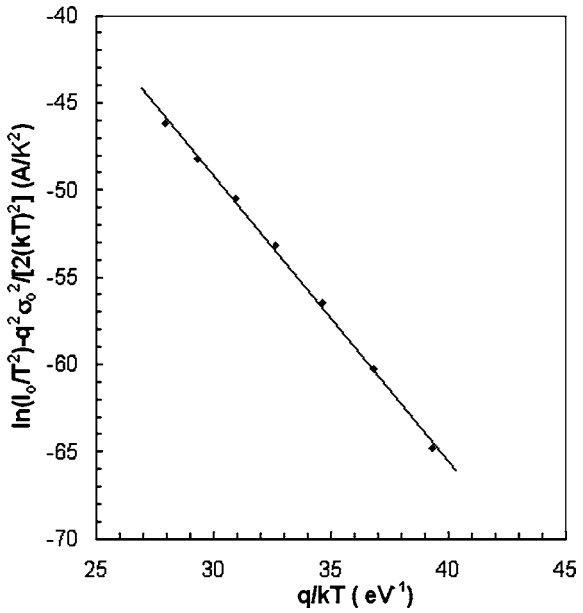

FIG. 9. Modified Richardson $\ln(I_0/T^2)-q^2\sigma_0^2/2(kT)^2$ versus q/kT plot for $(Ni/Au)-Al_{0.3}Ga_{0.7}N/AlN/GaN$ heterostructure according to the GD of BHs.

As can be seen, $\bar{\Phi}_{B0}=1.64$ eV from this plot [according to Eq. (13)], in agreement with the value of $\bar{\Phi}_{B0}=1.63$ eV from Φ_{ap} versus q/kT (Fig. 8). Therefore, it has been concluded that the temperature dependence of the forward *I-V* characteristics of the $(Ni/Au)-Al_{0.3}Ga_{0.7}N/AlN/GaN$ heterostructures can be successfully explained based on the TE mechanism with a GD of BHs.

IV. CONCLUSIONS

The forward bias *I-V* characteristics of the $(Ni/Au)-Al_{0.3}Ga_{0.7}N/AlN/GaN$ heterostructure were measured in the temperature range of 295–415 K. Using the evaluation of the experimental forward bias *I-V* characteristics reveals an increase of Φ_{B0} and a decrease of n with increasing temperature. Such behavior is attributed to the Schotky barrier inhomogeneities by assuming a GD of BHs due to barrier inhomogeneities that prevails at interface. In order to obtain evidence of a GD of BHs, we have drawn a Φ_{B0} versus q/kT plot, and the values of $\bar{\Phi}_{B0}=1.633$ eV and $\rho_0=0.215$ V for the mean barrier height and standard deviation at a zero bias, respectively, have been obtained from this plot. Then, the values of Φ_{B0} and A^* are obtained from a modified $\ln(I_0/T^2)-q^2\sigma_0^2/2(kT)^2$ versus q/kT plot as 1.618 eV and 34.25 $A/cm^2\,K^2$, respectively. The value of the Richardson constant of 34.25 $A/cm^2\,K^2$ is very close to the theoretical value of 33.74 $A/cm^2\,K^2$ (for undoped $Al_{0.3}Ga_{0.7}N$). For our sample, R_s is shown to play a crucial role in affecting the forward bias *I-V* curves of SBDs. The values of R_s show an unusual behavior, in which it increases with an increase of temperature. Moreover, the forward bias *I-V* curves show this behavior. This behavior of the crossing of *I-V* curves appears as an abnormality when seen with respect to the conventional behavior of SBDs.

ACKNOWLEDGMENTS

This work was supported by the Turkish State Planning Organization (Project No. 2001K120590) and the Gazi University BAP research projects (05/2006-30 and 05/2007-41). This work was also supported by TUBITAK under Project Nos. 104E090, 105E066, and 105A005. One of the authors (E.Ö.) also acknowledges partial support from the Turkish Academy of Sciences.

[1] T. Hashizume, S. Ootomo, S. Oyama, M. Konishi, and H. Hasegawa, J. Vac. Sci. Technol. B **19**, 1675 (2001).
[2] J. W. Johnson *et al.*, Solid-State Electron. **46**, 513 (2002).
[3] N. Miura *et al.*, Solid-State Electron. **48**, 689 (2004).
[4] T. Sawada, Y. Izumi, N. Kimura, K. Suzuki, K. Imai, S.-W. Kim, and T. Suzuki, Appl. Surf. Sci. **216**, 197 (2003).
[5] S. Çörekçi, M. K. Öztürk, B. Akaoğlu, M. Çakmak, S. Özçelik, and E. Özbay, J. Appl. Phys. **101**, 123502 (2007).
[6] T. Tut, N. Biyikli, I. Kimukin, T. Kartaloğlu, O. Aytur, M. S. Unlu, and E. Ozbay, Solid-State Electron. **49**, 117 (2005).
[7] D. J. As, S. Potthast, J. Fernandez, K. Lischka, H. Nagasawa, and M. Abe, Microelectron. Eng. **83**, 34 (2006).
[8] H. Hasegawa, Curr. Appl. Phys. **7**, 318 (2007).
[9] T. Sawada, Y. Ito, N. Kimura, K. Imai, K. Sukuzi, and S. Sakai, Appl. Surf. Sci. **190**, 326 (2002).
[10] Y. C. Lee, Z. Hassan, M. J. Abdullah, M. R. Hashim, and K. Ibrahim, Microelectron. Eng. **81**, 262 (2005).
[11] B. M. Green, K. K. Chu, E. M. Chumbes, J. A. Smart, J. M. Shealy, and L. F. Eastman, IEEE Electron Device Lett. **21**, 268 (2000).
[12] S. Zeyrek, Ş. Altındal, H. Yüzer, and M. M. Bülbül, Appl. Surf. Sci. **252**, 2999 (2006).
[13] T. Mizutani, Y. Ohno, M. Akita, S. Kishimoto, and K. Maezawa, Phys. Status Solidi A **194**, 447 (2002).
[14] T. Hashizume, S. Ootomo, and H. Hasegawa, Appl. Phys. Lett. **83**, 2952 (2003).
[15] H. Hasegawa, Y. Koyama, and T. Hashizume, Jpn. J. Appl. Phys., Part 1 **38**, 2634 (1999).
[16] C. R. Crowell and S. M. Sze, J. Appl. Phys. **36**, 3212 (1965).
[17] H. C. Card and E. H. Rhoderick, J. Phys. D **4**, 1589 (1971).
[18] Ş. Altındal, S. Karadeniz, N. Tuğluoğlu, and A. Tataroğlu, Solid-State Electron. **47**, 1847 (2003).
[19] İ. Dökme and Ş. Altındal, Semicond. Sci. Technol. **21**, 1053 (2006).
[20] S. M. Sze, *Physics of Semiconductor Devices*, 2nd ed. (Willey, New York, 1981).
[21] E. H. Rhoderick and R. H. Williams, *Metal Semiconductor Contacts*, 2nd ed. (Clarendon, Oxford, 1988).
[22] A. Tataroğlu, Ş. Altındal, and M. M. Bülbül, Microelectron. Eng. **81**, 140 (2005).
[23] P. Chattopadhyay and B. Raychaudhuri, Solid-State Electron. **35**, 605 (1993).
[24] S. Chand and J. Kumar, Semicond. Sci. Technol. **11**, 1203 (1996).
[25] S. Chand and J. Kumar, Appl. Phys. A: Mater. Sci. Process. **65**, 497 (1997).
[26] Ş. Karataş, Ş. Altındal, A. Türüt, and A. Özmen, Appl. Surf. Sci. **217**, 250 (2003).
[27] S. Zhu, R. L. Van Meirhaeghe, C. Detavernier, G. P. Ru, B. Z. Li, and F. Cardon, Solid State Commun. **112**, 611 (1999).
[28] J. H. Werner and H. H. Guttler, J. Appl. Phys. **69**, 1522 (1991).
[29] J. H. Werner and H. H. Guttler, Phys. Scr. **T39**, 258 (1991).
[30] H. Norde, J. Appl. Phys. **50**, 5052 (1979).
[31] K. Sato and Y. Yasamura, J. Appl. Phys. **58**, 3655 (1985).
[32] S. K. Cheung and N. W. Cheung, Appl. Phys. Lett. **49**, 85 (1986).
[33] H. Kim, M. Schuette, H. Jung and J. Song, Appl. Phys. Lett. **89**, 053516 (2006); A. J. Sierakowski and L. F. Eastman, J. Appl. Phys. **86**, 3398 (1999).
[34] J. Osvald and Zs. J. Horvath, Appl. Surf. Sci. **234**, 349 (2004).
[35] S. Chand and S. Bala, Semicond. Sci. Technol. **20**, 1143 (2005); S. Chand, *ibid.* **19**, 82 (2004).
[36] S. Chand and S. Bala, Appl. Surf. Sci. **252**, 358 (2005).
[37] J. Osvald, Solid State Commun. **138**, 39 (2006).
[38] Zs. J. Horvath, L. Dozsa, O. H. Krafcsik, T. Mohacsy, and Gy. Vida, Appl. Surf. Sci. **234**, 67 (2004).

[39]Ş. Altındal, H. Kanbur, D. E. Yıldız, and M. Parlak, Appl. Surf. Sci. **253**, 5056 (2007).
[40]B. Cvikl, D. Korosak, and Zs. Horvath, Vacuum **50**, 385 (1998).
[41]Y. P. Song, R. L. Van Meirhaeghe, W. H. Laflere, and F. Cardon, Solid-State Electron. **29**, 633 (1986).
[42]Zs. J. Horvarth, Solid-State Electron. **39**, 176 (1996).
[43]J. P. Sullivan, R. T. Tung, M. R. Pinto, and W. R. Graham, J. Appl. Phys. **70**, 7403 (1991).
[44]R. F. Schmitsdorf, T. U. Kampen, and W. Mönch, Surf. Sci. **324**, 249 (1995).
[45]R. T. Tung, Appl. Phys. Lett. **58**, 2821 (1991); Phys. Rev. B **45** 13509 (1992).